Streamlined Modeling for Characterizing Spacecraft Anomalous Behavior

Bernie Klem and Dave Swann

Aerospace Testing Alliance
Advanced Missile Signature Center
Arnold Engineering Development Center
Arnold AFB, TN

For presentation at the
AMOS Technology Conference

September 13 - 16, 2011

ABSTRACT

Anomalous behavior of on-orbit spacecraft can often be detected using passive, remote sensors which measure electro-optical signatures that vary in time and spectral content. Analysts responsible for assessing spacecraft operational status and detecting detrimental anomalies using non-resolved imaging sensors are often presented with various sensing and identification issues. Modeling and measuring spacecraft self emission and reflected radiant intensity when the radiation patterns exhibit a time varying reflective glint superimposed on an underlying diffuse signal contribute to assessment of spacecraft behavior in two ways: (1) providing information on body component orientation and attitude; and, (2) detecting changes in surface material properties due to the space environment. Simple convex and cube-shaped spacecraft, designed to operate without protruding solar panel appendages, may require an enhanced level of preflight characterization to support interpretation of the various physical effects observed during on-orbit monitoring. This paper describes selected portions of the signature database generated using streamlined signature modeling and simulations of basic geometry shapes apparent to non-imaging sensors. With this database, summarization of key observable features for such shapes as spheres, cylinders, flat plates, cones, and cubes in specific spectral bands that include the visible, mid wave, and long wave infrared provide the analyst with input to the decision process algorithms contained in the overall sensing and identification architectures. The models typically utilize baseline materials such as Kapton, paints, aluminum surface end plates, and radiators, along with solar cell representations covering the cylindrical and side portions of the spacecraft. Multiple space and ground–based sensors are assumed to be located at key locations to describe the comprehensive multi–viewing aspect scenarios that can result in significant specular reflection from both the sun and the underlying earth surface. The objects are modeled to be either tumbling or spin stabilized at key orientations in order to capture the complexity of the solar/earth incident illumination and the sensor viewing aspect conditions. Although these geometries and processes appear to be specialized and limited, they are sufficient to capture the principal observable features that are necessary for gaining insight into the complex issues of interpreting non-imaging sensor signals for monitoring the actual on-orbit spacecraft behavior changes. This talk has been prepared as a poster paper, to allow for engagement with conference participants on the presentation contents, and discussions for expansion of the material to include additional topical areas for future work, as appropriate. All discussions have been limited only to topics that could be discussed in the open format of the conference.

1. INTRODUCTION

The optical signatures presented in this paper represent the inherent radiant intensity apparent to a remote passive sensor for a baseline set of generic object shapes. The signatures have been generated using a low-to-moderate fidelity electro-optical signatures code that efficiently permits estimation of an object's maximum intensity along with representative values of the departure from that maximum value as the object orientation changes throughout its oscillation cycle.

Because we are dealing with the intensity parameter, sensor to object range is not an issue in non-resolved signature value. However, other parameters, such as the environment irradiation scenario and viewing aspect angles, can play a major role in the signature level as well as with the location of the object with respect to the complex earth scene irradiation pattern.

Since this objective was to generate a representative database of maximum values (with reasonable variations), sensor observation and environmental condition scenarios were established using a single set of conditions that are conducive to the plan described in the following section. Thus, for all conditions of this database, the sensor is assumed to be at the local horizon to the earth surface with the sun positioned behind the sensor so as to create a maximum illumination – observation phase

condition. The sensor views the object through this complete phase oscillation cycle against a pristine natural background with atmospheric attenuation not being an issue.

The objects are based on simple geometrical surfaces, possessing a fair degree of symmetry, with surface material properties that capture both the extreme values of environmental reflection and thermal self emission, and also a reasonable representation of realistic material property behavior. The spectral bands used in the calculations are square band generic visible, medium wave infrared, and long wave infrared bands that accurately simulate the reflective and emissive nature of the object's signatures. Careful review of the database features and results should provide the reader with comprehensive insight to performing more complex object geometry signature modeling with high fidelity simulation modeling tools.

This information summary has been designed to focus on object signature characterization. Specific references to topics and associated discussions related to sensor capability to detect, track, and identify the object with specific performance metrics such as detection range, signal to noise, etc. have been deferred to follow-on presentations.

2. WORK DESCRIPTION

The objective was to generate optical signatures using streamlined thermal-geometry models of fundamental object shapes (e.g. spheres, plates, cubes, cylinders, cones and composite cylinders with plates). This was accomplished using representative pure diffuse reflective and pure specular reflective components, representative surface emittances, and nominal to extreme values of surface temperatures. Included are cases for which, given the numerical reflectance values, the reflectance is modeled as a mixture of both 50% diffuse and 50% specular. Predictive signatures were generated in three generic spectral bands for a nominal environmental irradiation – sensor observation scenario. This generation included maximum value signatures as well as the angular dependent values throughout a complete object oscillation cycle.

3. STREAMLINED MODELING SIMULATIONS CONDITIONS

The object Geometry Models included a sphere, flat plate, cube, right circular cylinder, cone, and cylinder with an attached plate. The surface materials were limited to an Aluminum-type and a Silica-type. The scenarios had the objects located at geo altitude above earth surface and irradiated by the sun positioned at the horizon and underlying earth – cloud scene. The sensor is assumed to view the objects rotating through a complete oscillation cycle in the sun – sensor plane with the sun located directly behind them in generic visible (0.4 – 0.9 μm), MWIR (3.0 – 5.0 μm), and LWIR (8.0 – 12.0 μm) spectral bands. The simulation output included the object's inherent radiant intensity vs. the rotation angle, with 10 degrees resolution.

4. ANALYSIS RESULTS

The signature generation results are summarized in the sections below for the seven classes of object shapes modeled.

4.1 Sphere

The sphere was modeled to always present a projected area of 1 square meter (diameter = 1.128 m). The emittance was 0.5, the pure diffuse reflectance was 0.5, and the pure specular reflectance used was 0.5. The surface temperature was 280K. To account for realistic material reflectance properties the mixed reflectance was modeled as partially diffuse and partially specular, both with reflectance values of 0.25.

Signature results for modeling this object are presented in Figure 1. The plots represent the sphere radiant intensity in three spectral bands for the various material property characteristics. The constant intensity levels are appropriate to the observation - illumination scenario. Altering the position of the sun and the sensor will result in significant changes in the relative values of the curves for the visible and MWIR bands. Self emission dominates in the LWIR band.

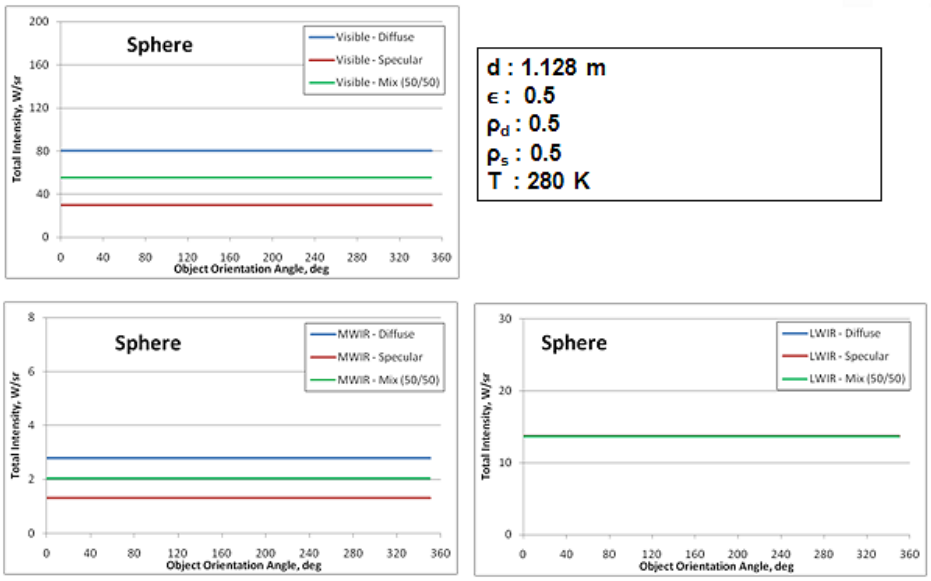

Fig. 1: Sphere Optical Signatures Modeling Results

4.2 Circular Plate

The circular plate was modeled to present a maximum projected area of 1 square meter (diameter = 1.128 m). The emittance was 0.5, the pure diffuse reflectance was 0.5, and the pure specular reflectance used was 0.5. The surface temperature was 280K. To account for realistic material reflectance properties the mixed reflectance was modeled as partially diffuse and specular, both with reflectance values of 0.25.

Signature results for modeling this object are presented in the Figure 2. The graphs represent the circular plate radiant intensity in three spectral bands for the various material property characteristics. The highly variable intensity levels are appropriate for the observation – illumination scenario. Altering the position of the sun and the sensor will result in significant changes in the relative values of the curves for the visible and MWIR bands. Zero intensity levels result from edge-on viewing of the plate, while self emission dominates in the LWIR band. The sharp spikes at orientation angles of 0 and 180 deg tend to over-emphasize the magnitude of the solar glint from the plate. Real material properties would display an angular broadening of this spike with a lower peak intensity value. Note that the solar glint also occurs in the LWIR.

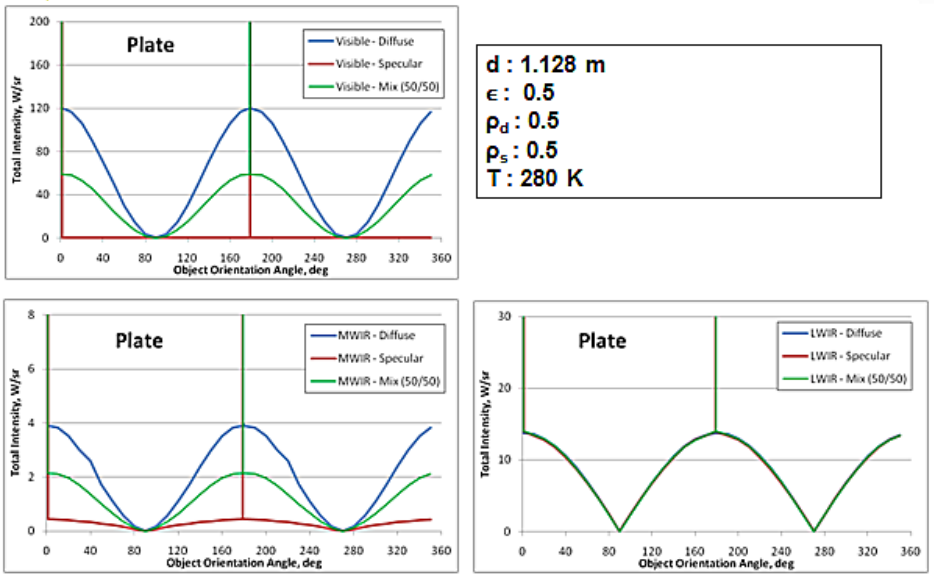

Fig. 2: Circular Plate Optical Signatures Modeling Results

4.3 Approximate Cube

This shape was modeled to present a projected area of 1 square meter (diameter = 1.128 m) when viewing any one of the six side plates broadside. The emittance was 0.5, the pure diffuse reflectance was 0.5, and the pure specular reflectance used was 0.5. The surface temperature was 280K. To account for realistic material reflectance properties the mixed reflectance was modeled as partially diffuse and specular, both with reflectance values of 0.25. The term "approximate" is used to describe the cube since the actual geometry was based on combining six circular plates, each of 1.128 m diameter. This process was used based on an inherent limitation of the streamlined modeling code.

Signature results for modeling this object are presented in Figure 3. The plots represent the cube radiant intensity in three spectral bands for the various material property characteristics. Because of the cube geometry reflection the intensity pattern remains fairly constant in the visible and MWIR, while the self emission LWIR shows more of a variation which may be due to the approximation of using composite plate sides in the modeling. Specular solar glinting is significant in all three bands whenever the orientation angle presents the full-phase viewing angle perspective to the sensor. As in the case of the circular plate, a slight reorientation of the object in the azimuth direction is expected to eliminate the specular component from the total signature.

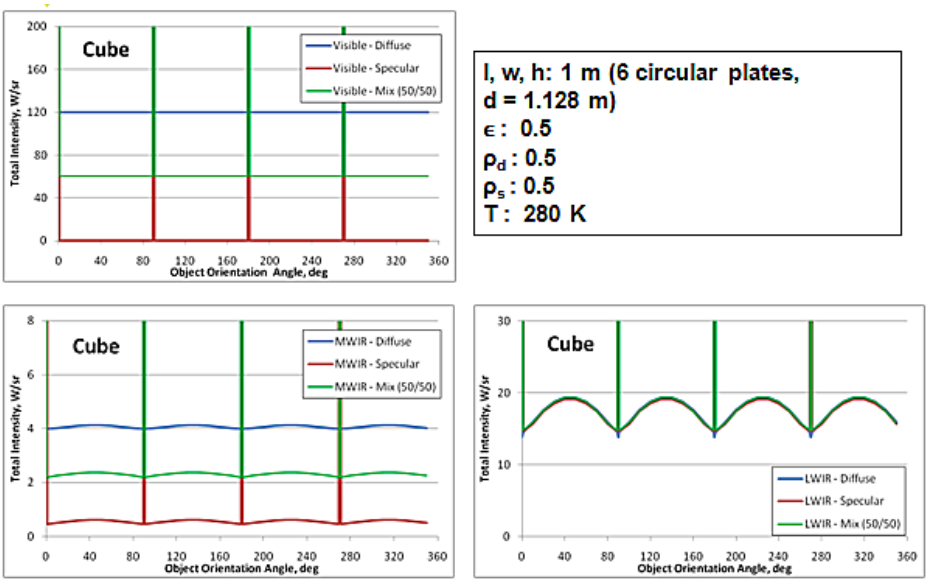

Fig. 3: Approximate Cube Optical Signatures Modeling Results

4.4 Cylinder

This shape was modeled as a right circular cylinder to present a maximum projected area of 1 square meter (length = 1 m, diameter = 1 m) when viewing the frustum broadside. For broadside viewing of the cylinder end plates the projected area was less than 1 square meter. For all surfaces, the emittance was 0.5, the pure diffuse reflectance was 0.5, and the pure specular reflectance used was 0.5. The surface temperature was 280K. To account for realistic material reflectance properties the mixed reflectance was modeled as partially diffuse and specular, both with reflectance values of 0.25.

Signature results for modeling this object are presented in Figure 4. The plots represent the cylinder radiant intensity in three spectral bands for the various material property characteristics. Because of the cylinder geometry reflection the intensity pattern remains fairly constant in the visible and MWIR, while the self emission LWIR shows more of a variation which may be due to the different projected areas between the frustum and the end plates. Specular solar glinting is significant in all three bands whenever the orientation angle presents the full-phase viewing angle perspective to the sensor. As in the case of the circular plate, a slight reorientation of the object in the azimuth direction is expected to eliminate the specular component from the total signature for the end plate maximum area viewing. Specular glint from the convex surface is a more complex situation. Note that the overall intensity levels are similar to those of the cube.

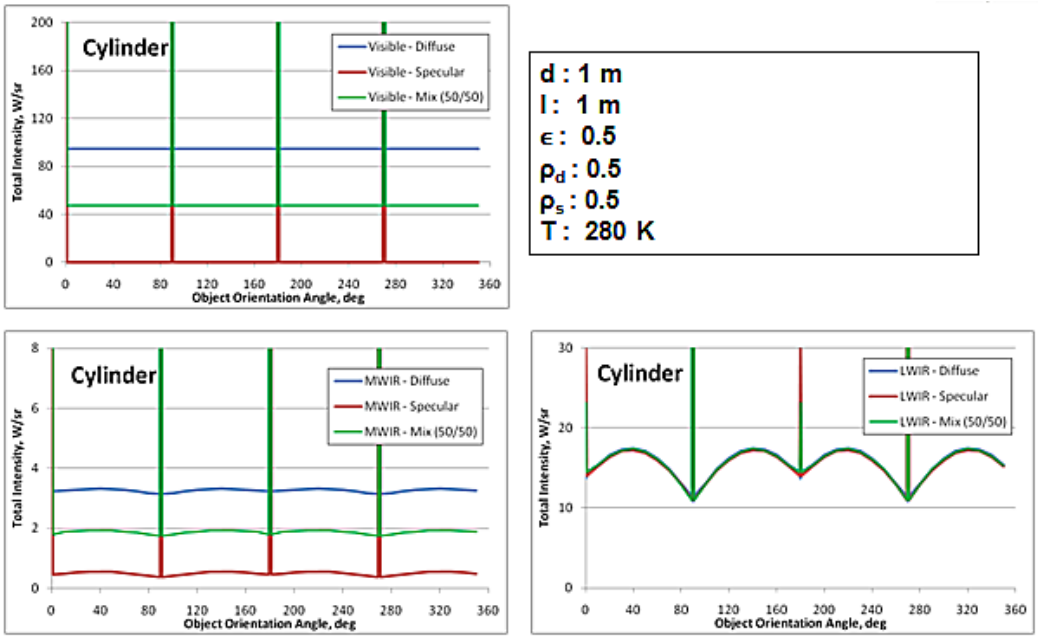

Fig. 4: Cylinder Optical Signatures Modeling Results

4.5 Small and Large Cones

The cones were modeled to present near maximum projected areas of 0.5 square meter (length = 1 m, diameter = 1 m) and 1.0 square meter (length = 2 m, diameter = 1 m) when viewing the frusta broadside. For all surfaces, the emittance was 0.5, the pure diffuse reflectance was 0.5, and the pure specular reflectance used was 0.5. The surface temperature was 280K. To account for realistic material reflectance properties the mixed reflectance was modeled as partially diffuse and specular, both with reflectance values of 0.25.

Signature results for modeling the small and large cones are presented in Figures 5 and 6. The graphs represent the radiant intensity in three spectral bands for the various material property characteristics. Of primary interest is the different intensity patterns obtained with orientation angle just by doubling the length of the cone while keeping all other parameters the same. Specular solar glinting is significant in all three bands whenever the orientation angle presents the full-phase viewing perspective of the base surface to the sensor. As in the case of the circular plate, a slight reorientation is expected to eliminate the base specular component from the total signature. Specular glints from the convex surface are a more complex situation. These are known to exist but the streamlined code used in the calculations could not generate data on these glints due to higher fidelity spatial and motion modeling limitations. Neglecting these glints is not expected to have a significant impact on the utility of this database; however there are plans to include them at a later date using modified versions of the present code or a different code possessing an inherent higher degree of modeling capability and fidelity.

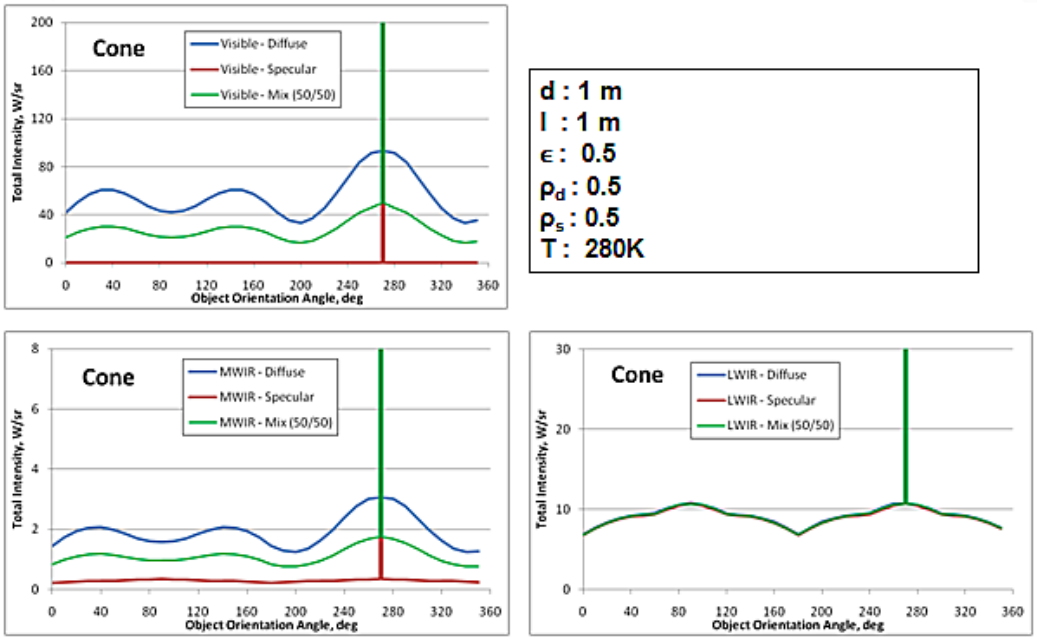

Fig. 5: Small Cone Optical Signatures Modeling Results

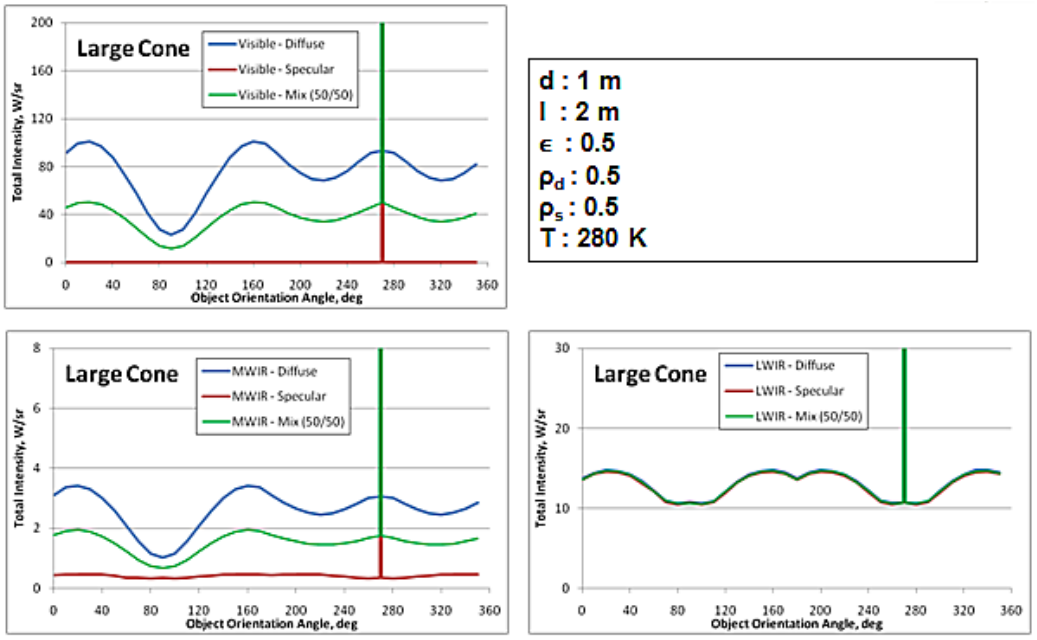

Fig. 6: Large Cone Optical Signatures Modeling Results

4.6 Complex Cylinder

This shape was modeled as a right circular cylinder to present a maximum projected area of 1 square meter (length = 1 m, diameter = 1 m) when viewing the frustum broadside. For broadside viewing of the cylinder end plates the projected area was less than 1 square meter. The emittance of the frustum was 0.78 and the end plates were 0.5, the diffuse reflectance was 0.07 for the frustum and 0.25 for the end plates. The specular reflectance was 0.15 for the frustum and 0.25 for the end plates. The surface temperature of the end plates was 280 K while the surface temperatures of the frustum were assumed to reach a maximum value of 330 K and a minimum of 220 K.

Signature results for modeling this object are presented in Figure 7. The graphs represent the cylinder radiant intensity in three spectral bands for a specific design in which the frustum contains a Silica-type material of variable temperature and the end plates are based on a constant temperature Aluminum-type surface. Results are presented for the extreme values of frustum temperature. Solar glinting is evident in all spectral bands for observations of both the end plates and the frustum with glint significantly reduced in the LWIR for some orientations. Reorientation of the object would be expected to eliminate the specular component to the total signature for the end plate maximum area viewing. Specular glint from the convex surface is a more complex situation and could persist for some other orientations. Note that the overall intensity levels are highly dependent on the surface temperature in the LWIR.

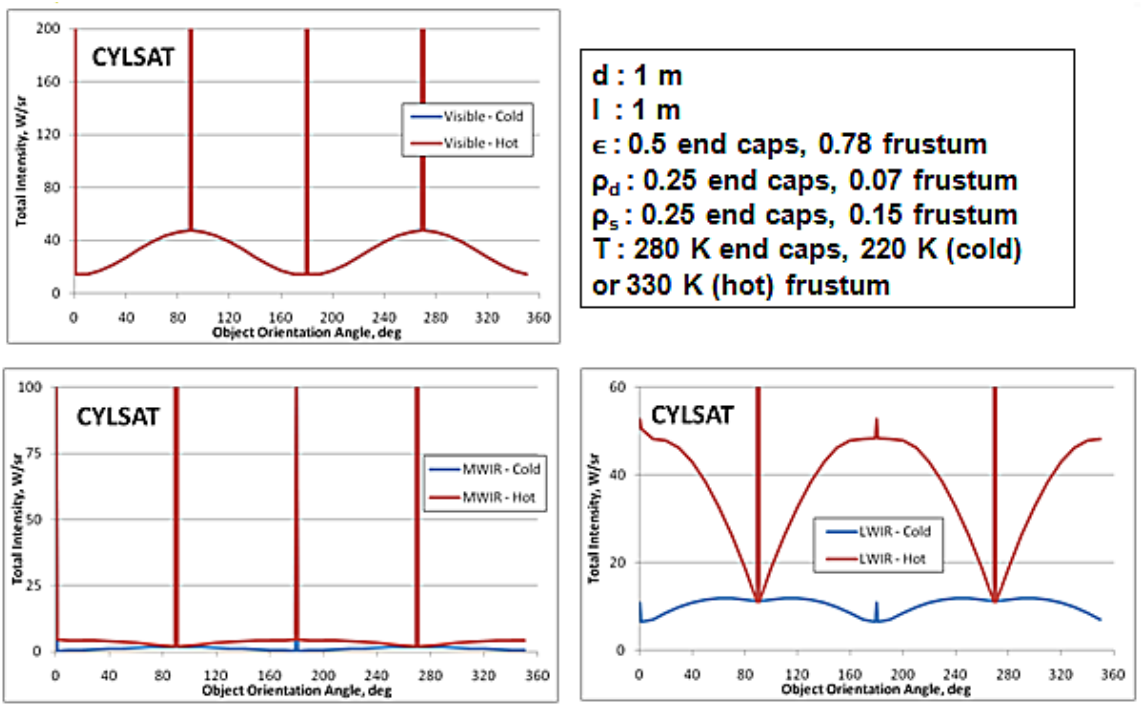

Fig. 7: Complex Cylinder Optical Signatures Modeling Results

4.7 Cylinder with Circular Plate

This shape was modeled as a combination of a 4 square meter maximum projected area (length = 4 m, diameter = 1 m) right circular cylinder and a 10 square meter (diameter = 3.568 m) circular plate so as to present a maximum projected area of 14 square meters, when viewing the co-aligned cylinder frustum and plate broadside. For the cylinder, the emittance was 0.5, the diffuse reflectance was 0.25, the specular reflectance used was 0.25, and the surface temperature was a constant 280 K. For the plate, the emittance was 0.78, the diffuse reflectance was 0.07, and the specular reflectance was 0.15. The surface temperature was assumed to reach a maximum value of 330 K and a minimum of 220 K.

Signature results for modeling this object are presented in Figure 8. The graphs represent the combination cylinder and plate radiant intensity in three spectral bands for a specific object design. This complex shape creates a highly angular dependent signature in all bands with consistent solar glint in these bands. When performing signature statistics database generation there needs to be awareness of these complex shape intensity patterns and consideration needs to be given to modeling this class of object under a more comprehensive set of scenario parameters. A major issue for this object is the characterization of signature with complete awareness of glint contributions from both the cylinder and the plate.

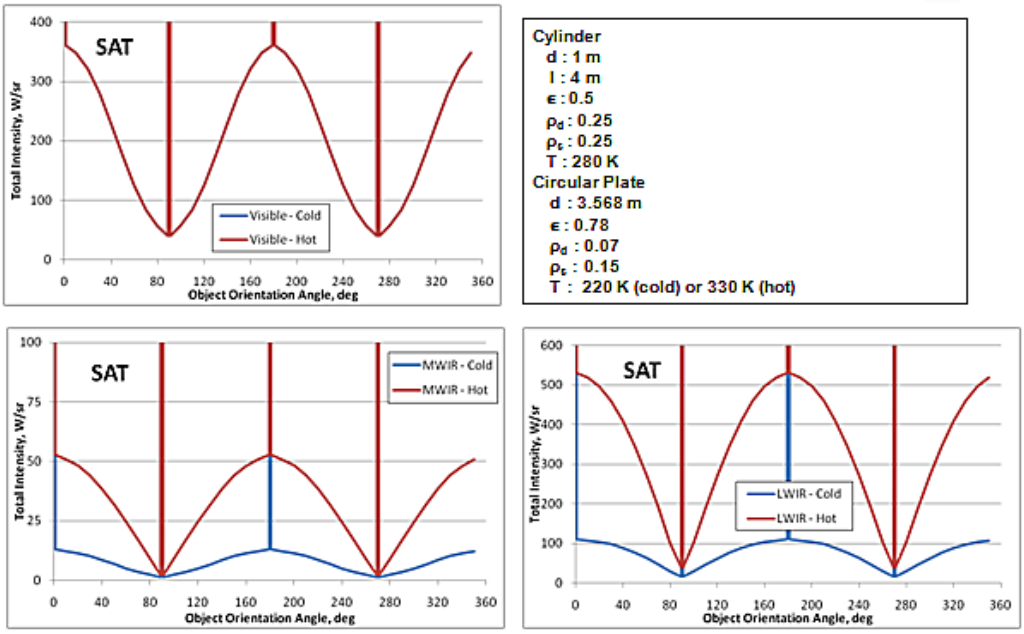

Fig. 8: Cylinder with Circular Plate Optical Signatures Modeling Results

5. SPECULAR GLINT SUMMARY

The large specular glint signature levels illustrated in the previous figures warrant special attention. This is evident in Table 1, which summarizes the specular glint intensities for the various shapes modeled during this activity. The table indicates the broad range of in-band intensities at various orientation viewing angles. To be noted is the relatively low level of specular signatures for the sphere as compared to the other object shapes of equivalent projected area. These appear to be from roughly three to six orders of magnitude difference. Not only is there significant glinting in the visible but also in both the MWIR and LWIR. Glint may persist or rapidly diminish with slight reorientation of the object and must be considered on a specific object shape basis. The peak value of the glint presented here is only an approximation and for real materials is reduced in magnitude but extended in angular width with flat surfaces behaving differently than curved surfaces. It should be apparent that consistent observations of objects under specific scenario conditions tend to enhance signatures for object tracking.

Table 1: Specular Glint Radiant Intensity (W/sr)

OBJECT	ORIENTATION	VIS	MWIR	LWIR
Sphere	All	30.0	1.3	13.7
Plate	Broadside	5.5×10^6	1.6×10^5	8.2×10^3
Cube	Broadside to all in-plane surfaces	5.5×10^6	1.6×10^5	8.2×10^3
Cone	Base View	4.4×10^6	1.3×10^5	6.4×10^3
Cylinder	End Plate Frustum	4.4×10^6 1.3×10^4	1.3×10^5 378	6.4×10^3 32.5
Cylsat				
Cold	End Plate Frustum	2.2×10^6 3.9×10^3	6.4×10^4 114	3.2×10^3 10.9
Hot	End Plate Frustum	2.2×10^6 3.9×10^3	6.4×10^4 118	3.2×10^3 52.7
Cyl + Plate				
Cold	End Plate Frustum	2.2×10^6 1.7×10^7	6.4×10^4 4.9×10^5	3.2×10^3 2.5×10^4
Hot	End Plate Frustum	2.2×10^6 1.7×10^7	6.4×10^4 4.9×10^5	3.2×10^3 2.5×10^4

6. ANALYSIS AND DISCUSSION

The results of this streamlined modeling effort provide good insight into object optical signature modeling fidelity needs for generating databases to support algorithm development for sensing, tracking, and identification architectures. It appears that basic shape object signature modeling tools of low-to-moderate fidelity can have utility as an initial process prior to generating detailed hi-fidelity models for specific object designs. Solar glint patterns and changes to diffuse signature patterns resulting from similar shaped object dimensional and material property details can introduce important issues in signature database utility (identification features). Although the results presented herein provide a reasonable estimate of object signature maximum values and their associated orientation variability, it would not be unreasonable to call upon the modeling tools used in this task to provide additional signature databases in the form of frequency of occurrence statistics. This would entail generating basic object signatures for a comprehensive range of object orientations with respect to a variable sun elevation – azimuth, sensor elevation – azimuth scenario. Object altitude above the earth surface may also be considered as a variable. Quite often, it is not necessarily a maximum or minimum signature level we are concerned with but rather the frequency with which a specific signature level can occur. Options are currently being assessed to compare results of selected object streamlined database signatures with results using hi-fidelity simulation tools.

7. ADDITIONAL MODELING OPTIONS AND ACTIVITY

During the time since this paper was prepared, work has continued in the following simulation areas and will be reported at a later date: A cylinder with circular plate system observed with slight azimuth rotation is being investigated. An approximate cube with construction characteristics similar to the complex cylinder case is being modeled for observations in nominal orientation and also with slight azimuth rotation. Also being looked at is the baseline, single material approximate cube observed with slight azimuth rotation. Plans include generating conical frustum surface specular glint patterns using an alternate low fidelity, higher angular resolution simulation tool.

8. SUMMARY

An optical signatures database was generated using streamlined thermal-geometry models of fundamental object shapes (e.g. spheres, plates, cubes, cylinders, cones and composite cylinders with plates). The database features included extreme reflectance, emittance, and temperature values. Results are applicable to the complete range of optical spectral band phenomenology. The process utilized an irradiation – observation scenario applicable to sizing maximum signature levels and reasonable variations.

A comprehensive set of object in-band inherent radiant intensity patterns were generated that demonstrates both constant and highly variable intensity levels, based on the specific object's geometrical and thermal characteristics. Results indicate frequent observances of solar glint at specific object orientation angles with respect to the sun and sensor, superimposed on underlying diffuse signatures. The process provides measures to compare different object shapes and material properties signature patterns with those of a diffuse spherical object for equivalent projected areas.

Results indicate that low fidelity signature modeling of the type used to generate this database can provide significant utility in object signature sizing prior to developing high fidelity signature models for advanced applications. Additional streamlined modeling of this type for these objects and one additional cubical design can provide useful information on the sensitivity of observing specular glints for alternative object orientations and observation-irradiation scenarios.